Defence Science Journal, Vol. 64, No. 3, May 2014, pp. 309-313, DOI : 10.14429/dsj.64.7329

Influence of Temperature on the Conformational Guided Physical Properties of Ultrathin Films of PLLA

Pallavi Pandit, Mandira Banerjee[*], G.S. Mukherjee[#], Rakesh Parikh[@], U.P. Deshpanday[!], and Ajay Gupta[$]

School of Physics, Devi Ahilya University, Indore-452 001, India
[#]Defence Scientific Information and Documentation Centre, DRDO, New Delhi-110 054, India
[@]Raja Ramanna Centre for Advanced Technology, Indore-452 013, India
[!]UGC-DAE, Consortium for Scientific Research, Indore-452 001, India
[$]Center for Spintronic Materials, Amity University, Noida-201 303, India
[*]E-mail: mandira_bm@rediffmail.com

ABSTRACT

Poly (L lactic acid) (PLLA) ultrathin films of various thicknesses were prepared by spin coating method and investigated by using vibrational spectroscopic techniques such as FTIR and Raman. The analysis has been done in two parts: first one is verification of structural mode to understand the visibility of characteristic band to confirm the PLLA structure; where interestingly, as the thickness of the film increased, the structural features were found to be more explicit. The second part of the study was to observe the features of the film having been annealed for 1 h in two separate temperatures, one at specific annealing temperature 120 °C and the other at 160 °C to enable PLLA chains to reorient to get crystallized from its soften state at two such specific temperatures. The isothermal crystallization behavior of PLLA film at 120 °C and 160 °C from the melt was monitored by FTIR as well as Raman spectroscopies. More importantly, the band at 921 cm^{-1} corresponds to α crystalline phase of PLLA has been observed even in this ultrathin film with the effective application of temperature as selected in this study.

Keywords: Ultrathin film, biopolymer, X-ray reflectivity, PLLA

1. INTRODUCTION

Ultrathin films are becoming important from the point of view of both basic physics and technology. Among the family of environmental friendly biodegradable polymers, poly (L lactic acid), PLLA (-[$CH_2CH(CH_3)COO]_n$-) - has been attracting much attention because of many advantages in its intrinsic properties. For example, the polymer exhibits biocompatibility[1-3], and so has importance in medical industry for applications such as drug delivery systems, implant materials for bone fixation[4], nuclear oncology and surgical suture[5-15]. But the main reason behind its debut in large-scale production is found in its tremendous potential in traditional applications where thermoplastics are employed, such as the production of disposable products for the packaging and film industries[16]. PLLA is also melt-spinable and has very good fiber- and film-forming properties. Recently, applications involving high-strength fibers and films were reported[17]. But there is no detail of information prevalent in the literature on the role of annealing on the morphological state with reference to the vibration spectroscopic features. The objective of this study is to investigate the effect of annealing on the structural variation in the PLLA film. The morphology is observed by Fourier transform infrared (FTIR) and Raman measurement. The former is utilized to study the structural variation and the latter is to investigate the conformation of crystallite form with the effect of temperature. FTIR and Raman measurements on PLLA films mainly focused on the identification of characteristic bands[19-21].

2. EXPERIMENT

PLLA was procured from Sigma Aldrich and used in as-received form. The ultra thin films of PLLA (Mw-125, 000) were prepared by spin coating technique. Prior to deposition *Si* wafer was ultrasonically cleaned in acetone followed by iso-propanol and Milli-Q water (ca. 15 MΩcm). PLLA was dissolved in chloroform to make a uniform solution (70 mg/10 ml). After that PLLA thin film of different thicknesses were prepared by spin deposition technique by means of varying concentration and rpm rate. All films were grown under identical conditions in air on *Si* (100) substrate. Films of various thicknesses were prepared as 15 nm, 25 nm, 30 nm, and 40 nm films are designated as S_1, S_2, S_3 and S_4 respectively. For the purpose of study the effect of temperature on PLLA films, similar film of thickness circa 40 nm was also drawn on cleaned *Si* wafer coated with *Au* buffer layer. Film was grown under identical conditions in air (4000 rpm, 60 s) and is designated as S_5. To meet the requirement of standardization of surface analysis of the film, x-ray reflectivity experimental measurements have

Received 1 November 2013, revised 3 March 2014, online published 20 May 2014

been made using Bruker-AXS D8-Discover diffractometer equipped with a special reflectivity stage.

PLLA film (S_5) has been annealed at 120 °C and 160 °C for 1 h in each case to allow crystallization. FTIR spectrometer (Bruker Model Vertex 70 spectrophotometer) with attenuated total reflectance (ATR) attachment using ZnSe crystal was used to record the FTIR spectrum of the films of various thicknesses in range of 800 cm^{-1} to 1300 cm^{-1}. The data were recorded from 16 scans at 2 cm^{-1} resolution with correction for atmospheric water and carbon dioxide. Raman spectra were obtained using a Bruker Fourier transform Raman spectrometer (Horiba JYHR800 model). Surface morphology of the film with effect of temperature has been carried out by AFM using Nanoscope IV from DI-Veeco, USA.

3. RESULTS AND DISCUSSION

At the outset x-ray reflectivity experimental measurements were made using x-ray reflectivity (XRR) technique with an objective to determine thin film parameters including thickness, density and surface/interface roughness. Figure 1 depicts XRR pattern of the four films, as a function of momentum transfer vector *q*. The fitting of the experimental data was done using Parratt recursive formalism[18]. Best fitted values of thickness, roughness and electron density for all films are listed in Table 1. The total thickness as well as roughness of the films increases in going from sample S_1 to S_4. Clearly, such gradual increase in electron density of the film with their thickness but decrease in electron density per unit thickness, thus implicates formation of thin film in accordance with the trend to show its typical thin film characteristics.

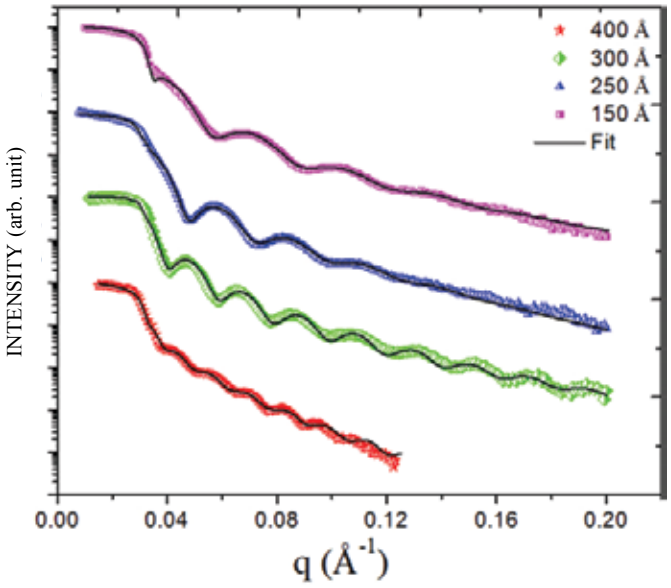

Figure1. X-ray reflectivity of PLLA films of various thicknesses as a function of momentum transfer vector q.

Efforts have been made to elucidate the structural features of PLLA thin films of various thicknesses (Fig. 2), along with isothermal crystallization behavior of S_5 (Fig. 3), which has been studied at two annealing temperatures 120 °C and 160 °C from the melt. The film with the minimum electron density S_5 was chosen for the studies using vibrational spectroscopy.

Table 1. Thickness, roughness and electron density of various PLLA films on *Si* (100) substrate

Sample	Layer thickness (nm)	Thin film roughness (nm)	Electron density (nm^{-3})	Electron density per unit thickness (nm^{-4}) x 10^{-2}
S_1	15	0.4	0.310	2.067
S_2	25	0.9	0.313	1.252
S_3	30	1.1	0.319	1.063
S_4	40	1.3	0.356	.0089

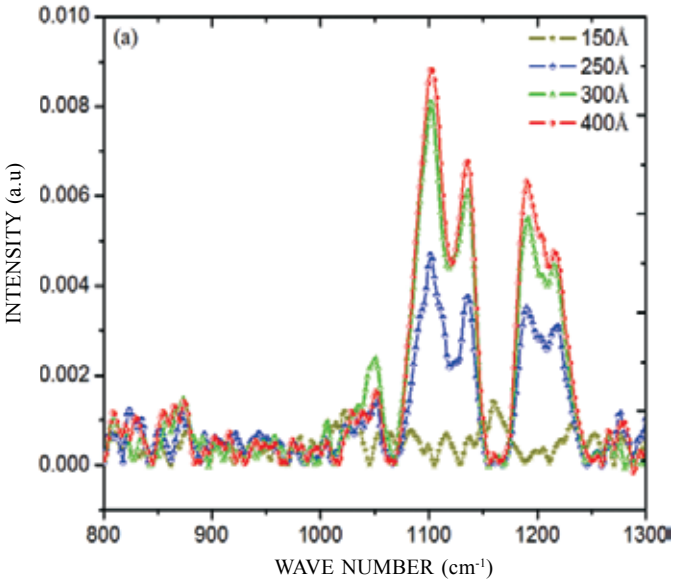

(a)

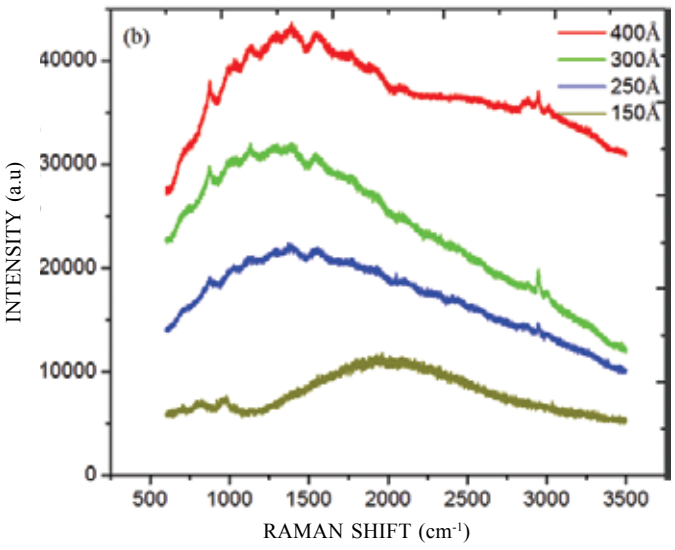

(b)

Figure 2. Spectroscopic results of various PLLA thin films of various thicknesses (a) FTIR spectra, (b) Raman s pectra.

In FTIR spectra, we have first investigated the spectral bands that confirm the identical form of PLLA; secondly we have examined the structural variation as an effect of temperature. Before we discuss the effect of temperature on

structure orientation of PLLA chain in ultrathin films with the FTIR data, it is necessary to summarize the characteristic bands of PLLA more explicitly associated with the orientation effect. For this purpose, we have collected the FTIR data of PLLA thin films. In the literature the PLLA films that were analyzed are of the order of few microns whereas in our case the films are having thickness of the order of few nano-meters. Therefore, it would be interesting to study the FTIR spectra of such ultra thin films to confirm their characteristic structure. Band positions as reported in literature[22,23] are listed in Table 2.

Table 2. FTIR Band assignments of PLLA in the 1300-1000 cm^{-1} region (18)

IR frequencies (cm^{-1})	Assignments
1268	$\nu(CH) + \nu(COC)$
1212	$\nu_{as}(COC) + r_{as}(CH_3)$
1182	$\nu_{as}(COC) + r_{as}(CH_3)$
1133	$r_s(CH_3)$
1089	$\nu_s(COC)$

where ν_{as}: asymmetric stretching, ν_s: symmetric stretching, r_s : rocking.

FTIR data is more overlapping in nature and generally gives first hand information of the relatively bulk system. FTIR spectra of sample S_1-S_4 are presented in Fig. 2(a). The structural bands in region 950 cm^{-1} - 1250 cm^{-1} are visible and quite matching with the earlier reported work, for which a detailed analysis has been made with a focus on the range of 1300 cm^{-1} - 800 cm^{-1} where bands are particularly overlapped. According to the band assignments in FTIR spectra, the 1182 cm^{-1} band is assigned to $\nu_{as}(C\text{-}O\text{-}C) + r_{as}(CH_3)$, and the bands at 1133 cm^{-1} are the pure band relative to the CH_3 group, $r_s(CH_3)$. The 1109 cm^{-1} band is due to ν_s (C-O-C), which is a pure band relative to the C-O-C backbone of PLLA. In the previously reported work, pointed out that the bands located around 1193 cm^{-1} and 1109 cm^{-1} are both sensitive to the C-O-C *trans* conformation in the crystalline phase of PLLA. The band at 1193 cm^{-1} is sensitive not only to the structural adjustment of the C-O-C backbone but also to the structural order of the CH_3 group. The information about the sequential changes of the bands at 1193 cm^{-1}, 1133 cm^{-1}, and 1109 cm^{-1} can be obtained from several well separated cross-peaks in Fig. 3 (a). Its shows the sequential order of intensity of these three bands is 1191 cm^{-1} < 1131 cm^{-1} < 1105 cm^{-1}, which is consistent with the varying thickness. The band positions of films are well matches with the earlier work[22]; this confirms that these ultra thin PLLA films are well formed.

Further a detailed analysis was carried out in order to get a better clarity in understanding the change. In correlation the Raman spectra have been recorded in region 550 cm^{-1} - 3500 cm^{-1} (Fig. 2(b)). The position of modes is similar in case of Raman spectra. Both the spectroscopic measurements verify the characteristic structure of PLLA.

To study the effect of temperature on the structure phase transition we have opted melt crystallization process on the S_5 film in which the electron density is minimum yet it's all the identical bands are visible. The band positions are shifted to some extent from bulk that may be due to the interaction of

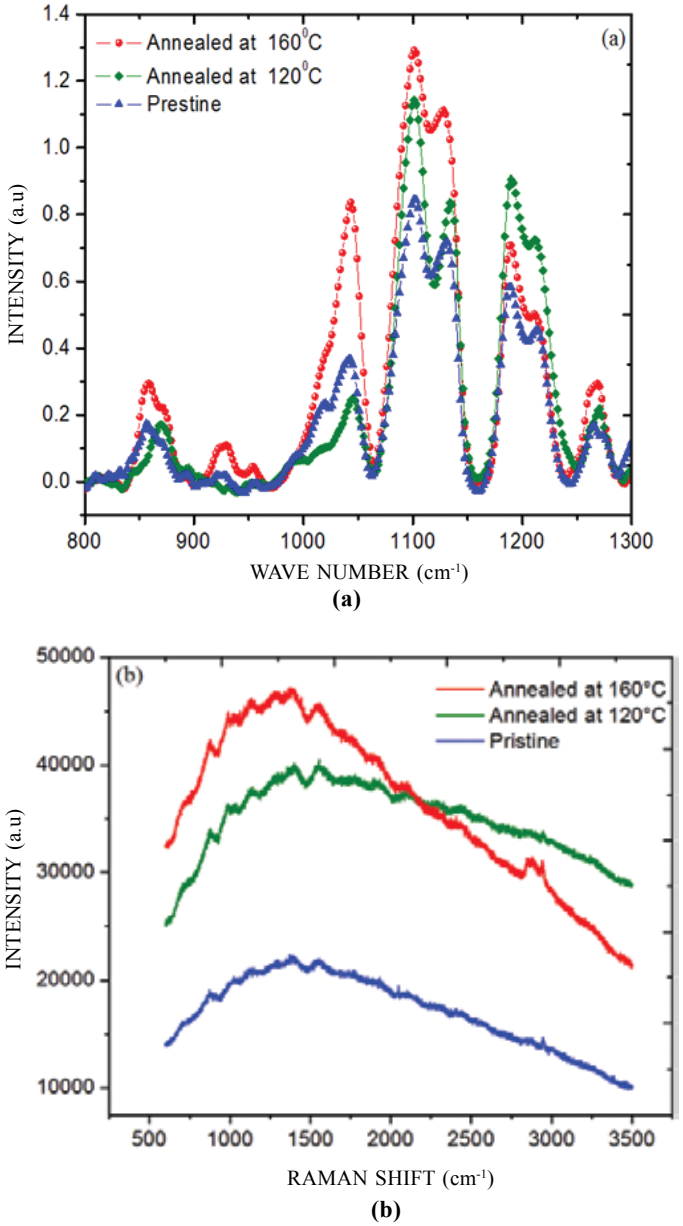

Figure 3. (a) FTIR Spectra and (b) Raman spectra of PLLA thin film annealed at 120 °C and 160 °C.

polymer to the surface of the substrate of *Au* buffer layer on *Si* (100) wafer in our case. For that the film is melted at 220 °C for 3 min - 4 min. then annealed at 120 °C and 160 °C for an hour in each case. FTIR and Raman spectrum of annealed film are shown in Fig. 3.

Here some structural variations are noticed which take place during the melt crystallization of PLLA; C-O-C stretching band region of 1300 cm^{-1} - 1000 cm^{-1}, and the skeletal stretching and CH_3 rocking band region of 970 cm^{-1} - 850 cm^{-1}. Kister[23], *et al.* and Cohn[24], *et al.* reported FTIR of PLLA thin film (~μm). The band at 921 cm^{-1} is characteristic helical sensitive α crystalline band of PLLA. This band assigned to coupling of the C-C backbone stretching and CH_3 rocking mode, sensitive to the 10_3 helix chain conformation of PLLA α crystals. Along with it, a band at 871 cm^{-1} is also sensitive

to the 10_3 helix conformation. Jianming[25], *et al.* suggested the other two crystallization-sensitive bands at 957 cm^{-1} and 857 cm^{-1}; however, on the other hand the region of 970 cm^{-1} - 850 cm^{-1} represents more of amorphous state of PLLA. These characteristic bands are observed in PLLA films in the present case also.

FTIR spectrum of the PLLA film before annealing shows the major contribution of amorphous band at 957 cm^{-1} and 857 cm^{-1} more than the crystalline band at 921 cm^{-1} and 871 cm^{-1}. Interestingly, in our case the intensities of the bands at 921 cm^{-1} and 871 cm^{-1} increase with temperature of annealing, while the intensity of bands at 957 cm^{-1} and 857 cm^{-1} decrease that shows the film is actually in semi crystalline form. It suggests that the sample prepared from the melt crystallization was initially in the amorphous state, and α crystal form of PLLA films was formed after annealing at 120 °C and 160 °C.

Additionally 1300 cm^{-1} to 800 cm^{-1} region is reportedly highly sensitive to the crystallization process hence in this study, we are particularly interested in this region. As the crystallization progresses at 120 °C and 160 °C, the intensities of some bands change greatly, and the others show a frequency shift. In the range of 1300 cm^{-1} - 1000 cm^{-1}, usually, the fundamental modes of a single polymer chain are split into various spectral components in the crystal if the intermolecular forces between polymer chains are sufficient enough. Polymers not only exhibit resonance splitting of bands associated with interaction between analogous groups along the polymer chain but also show splitting of certain vibrations related to intermolecular interaction because of the helical chain structure. The splitting of $\nu_{as}(CH_3)$ can be clearly observed in S_5 sample before and after annealing, which indicates that the CH_3 groups among PLLA chains are already in close contact prior to the crystal growth in PLLA; Fig. 3 supports such manifestation.

Some characteristic bands are associated with crystalline phase of the material whereas some bands represents amorphous phase of the material[23,26]. The bands at 1182 cm^{-1}, 1205 cm^{-1}, and 1212 cm^{-1} representing amorphous state of the PLLA, are assigned to the combination of ν_{as}(C-O-C) and $r_{as}(CH_3)$. In the crystalline state, the band at 1212 cm^{-1} shifts to 1215 cm^{-1}, whereas the band at 1183 cm^{-1} splits into two bands at 1194 cm^{-1} and 1184 cm^{-1}. A similar case can also be seen in the (C-O-C) region, where only one band appears at 1089 cm^{-1} for the amorphous state, but two bands are observed at 1107 cm^{-1} and 1089 cm^{-1} for the crystalline state. Moreover, the band intensities around 1194 cm^{-1} and 1107 cm^{-1} increase with the annealing temperature (Fig. 3(a)). The characteristic bands of PLLA are more intense in case of thick films as compared to thinner film which can be seen in the FTIR as well as Raman spectra in Fig. 2. It is worthy to note that some of the bands which were not clearly seen in film of lower thickness were clearly visible in higher thickness films.

In the present work, one can see in Fig. 2 that with increasing thickness the intensity of absorption bands increases. In melt crystallization process opted for S_5, the intensity of crystalline bands increases while the intensity of amorphous band decreases with the effect of temperature of annealing as shown in Fig. 3.

The spectral change in evidence to the effect of melt crystallization process is confirmed by the Raman Spectroscopy. Clear peaks corresponding to various modes are observed. It may be noted that for FTIR the convenient range for study was found 1300 cm^{-1} to 800 cm^{-1} whereas for Raman study the convenience lies in the range 3000 cm^{-1} - 500 cm^{-1}. More importantly, along with the spectral modes in Raman the region 2800 cm^{-1} - 3000 cm^{-1} has been clearly separated in both the thin films proceed with melt crystallization process.

AFM of the PLLA film was recorded to observe the actual surface topography of the annealed film. The typical feature of a representative PLLA film is shown in Fig. 4. It is worthy to note that even in the ultrathin film such crystalline domains are visible. Nucleation growth represents the crystallize structure of the film.

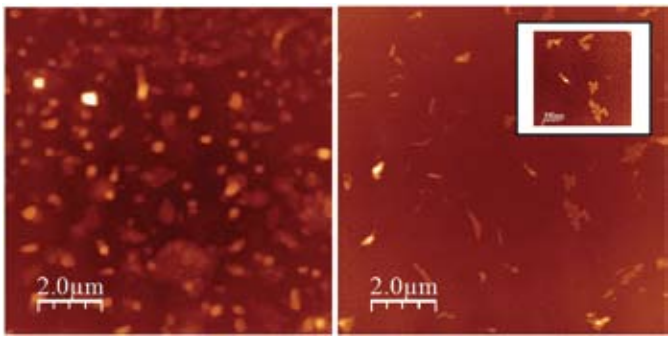

Figure 4. AFM image of PLLA thin film :As-deposited film (left) and after annealing at 160 °C (right).

4. CONCLUSIONS

In the present study, we have investigated the effect of thickness of thin film along with isothermal crystallization behavior of PLLA thin film at 120 °C and 160 °C from melts by FTIR as well as Raman spectroscopy. To elucidate the intermolecular interaction, before and after annealing, the skeletal stretching and CH_3 rocking bands in the 1300 cm^{-1} - 800 cm^{-1} region were investigated by IR analysis. It has been found that both the crystalline bands at 921 cm^{-1} and 871 cm^{-1}, that are related to the 10_3 helix conformation of PLLA are clearly visible in annealed sample that confirms the crystallized structure of the film.

ACKNOWLEDGEMENTS

Authors are thankful to UGC-DAE, CSR, Indore for providing research facilities and financial assistance. Thanks are due to Mr Manoj Kumar for Raman measurements and Mr Mohan Gangrade for AFM measurements.

REFERENCES

1. Luczynski, K.W.; Brynk, T.; Ostrowska, B.; Swieszkowski, W.; Reihsner, R. & Hellmich, C. Consistent quasistatic and acoustic elasticity determination of poly-l-lactide-based rapid-prototyped tissue engineering scaffolds. *J. Biomed. Mater. Res. A*, 2013, **101**, 139–144.
2. Liu, Y.S.; Huang, Q.L.; Kienzle[c], A; Müller[c], W.E.G. & Feng, Q.L. In vitro degradation of porous PLLA/pearl powder composite scaffolds. *Mater. Sci. Eng. C,* 2014, **38**, 227–234.
3. Thangaraju, E.; Srinivasan, N.T.; Kumar, R.; Sehgal,

P.K. & Rajiv, S. Fabrication of electrospun poly l-lactide and curcumin loaded poly l-lactide nanofibers for drug delivery. *Fibers Polym*., 2012, **13**(7), 823–830
4. Nguyen, T.H. & Lee, B.T., In vitro and in vivo studies of rhBMP2-coated PS/PCL fibrous scaffolds for bone regeneration. *J. Biomed. Mater. Res. A,* 2013, **101**, 797–808
5. Ikada, Y. &Tsuji, H. Biodegradable polyesters for medical and ecological applications. *Macromol. Rapid Commun*., 2000, **21**(3), 117-132.
6. Tsuji, H. & Ikada, Y. *J. B*lends of aliphatic polyesters. II. Hydrolysis of solution-cast blends from poly(L-lactide) and poly(E-caprolactone) in phosphate-buffered solution. *Appl. Polym. Sci.,* 1998, **67**(3), 405-415.
7. Tsuji, H. & Ikada, Y. Crystallization from the melt of poly(lactide)s with different optical purities and their blends. *Macromol. Chem. Phys.,* 1996, **197**(10), 3483-99.
8. Urayama, H.; Kanamori, T. & Kimura, Y. Properties and Biodegradability of Polymer Blends of Poly(L-lactide) s with Different Optical Purity of the Lactate Units. *Macromol. Mater. Eng.,* 2002, **287**(2), 116-121.
9. Dorgan, J. R. Poly(lactic acid) Properties and Prospects of an EnVironmentally Benign Plastic; American Chemical Society: Washington, DC, 1999, pp.145-149.
10. Lunt, J. Large-scale production, properties and commercial applications of polylactic acid polymers. *Polym. Degrad. Stab*. 1998, **59**(1-2), 145-152.
11. Zhu, K. L.; Xiangzhou, L. & Shilin, Y. Preparation, characterization, and properties of polylactide (PLA)–poly(ethylene glycol) (PEG) copolymers: A potential drug carrier. *J. Appl. Polym. Sci*. 1990, **39**(1), 1-9.
12. Bergsma, J. E.; Bos, R. R. M.; Rozema, F. R.; Jong, W. D. & Boering, G. Biocompatibility of intraosseously implanted predegraded poly(lactide): an animal study *J. Mater. Sci.: Mater. Med.* 1996, **7**(1), 1-7.
13. Nijsen, J.F.W.; van het Schip, A.D.; Hennink, W.E.; Rook, D.W.; van Rijk, P.P. & de Klerk, J.M.H. Advances in nuclear oncology: microspheres for internal radionuclide therapy of liver tumours. *Curr. Med. Chem.,* 2002, **9**(1), 73–82.
14. Nijsen, J.F.W.; Zonnenberg, B.A.; Woittiez, J.R.W.; Rook, D.W.; Swildens-van Woudenberg, I.A.; van Rijk, P.P. & het Schip, A.D. Holmium-166 poly lactic acid microspheres applicable for intra-arterial radionuclide therapy of hepatic malignancies: effects of preparation and neutron activation techniques. *Eur. J. Nucl. Med.,* 1999, **26**(7), 699–704.
15. Fambri, L.; Pergoretti, A.; Fenner, R.; Incardona, S. D. & Migliarisi, C. Biodegradable fibres of poly(l-lactic acid) produced by melt spinning. *Polymer,* 1997, **38**(1), 79-85.
16. Sinclair, R. G. The case for polylactic acid as a commodity packaging plastic. *Pure Appl. Chem.,* 1996, **33**(5), 585-97.
17. Hoogsteen, W.; Postema, A. R.; Pennings, A. J.; Brinke, G. T. & Zugenmaier, P. Crystal structure, conformation and morphology of solution-spun poly(L-lactide) fibers. *Macromolecules* 1990, **23**(2), 634-642.
18. Parratt, L. G. Surface studies of solids by total reflection of x-rays. *Phys. Rev. B,* 1954, **95**(2), 359-369.
19. Siegfried, Wartewig. IR and Raman Spectroscopy: Fundamental Processing. 2003, WILEY-VCH Verlag GmbH & Co. KGaA, Weinheim.
20. Laserna, J. J. (ed.) in Modern Techniques in Raman Spectroscopy (John Wiley & Sons, Chichester, 1996).
21. Banwell C. N. & Mccash, E. M. in Fundamentals of Molecular Spectroscopy (The McGraw-Hill Companies, London, 1994).
22. Zhang, Jianming; Tsuji, Hideto; Noda, Isao & Ozaki, Yukihiro. Structural changes and crystallization dynamics of poly(l-lactide) during the cold-crystallization process investigated by infrared and two-dimensional infrared correlation spectroscopy. *Macromolecules,* 2004, **37**(17), 6433-6439.
23. Kister, G.; Cassanas, G. & Vert, M. Effects of morphology, conformation and configuration on the IR and Raman spectra of various poly(lactic acid)s. *Polymer*, 1998, **39**(2), 267-273.
24. Cohn, D. & Younes, H. J.Biodegradable PEO/PLA block copolymers. *Biomed. Mater. Res.,* 1988, **22**(11), 993-1009.
25. Zhang, Jianming; Tsuji, Hideto; Noda, Isao & Ozaki, Yukihiro. Weak Intermolecular Interactions during the Melt Crystallization of Poly(l-lactide) Investigated by Two-Dimensional Infrared Correlation Spectroscopy. *Phys. Chem. B,* 2004, **108**(31), 11514-20.
26. Tsuji, H.; Ikada, Y. Stereocomplex formation between enantiomeric poly(lactic acid)s. XI. Mechanical properties and morphology of solution-cast films. *Polymer,* 1999, **40**(24), 6699-6708.

CONTRIBUTORS

Pallavi Pandit is a doctoral student from Devi Ahilya University, Indore, India. She has completed her MSc in 2003 from the same university and later worked as Research Intern at AMPRI, Bhopal, India during 2004 - 2008. Thereafter she joined as a CSIR Senior Research Fellow at DAVV, Indore. She is currently working in Collaborative Research Scheme of UGC-DAE Consortium for Scientific Research, India. Her expertise is in the field of soft condensed matter, in particular, metal organic LB films, polymer films and metal-polymer nano-composite films. She has also been a user of SAXS beamline at Stanford Synchrotron Radiation Light source, USA, SAXS beamline at Elettra Synchrotron, Trieste, Italy and EDXRD beamline at INDUS II, Indore, India.

Prof. Ajay Gupta is director of the Amity Center for Spintronic Materials, Amity University, Noida. Prior to this he was Center-Director of the Indore center of UGC-DAE Consortium for Scientific Research, from where he superannuated in May 2013. He was professor of Materials Science at Devi Ahilya University, Indore till 1994. His research interests include spintronic materials, magnetic thin films and multilayers, multiferroic materials, soft condensed matter. He has more than 300 research publications in peer-reviewed journals with about 2500 citations.